Multiscale Superpixel-Level Subspace-Based Support Vector Machines for Hyperspectral Image Classification

Article *in* IEEE Geoscience and Remote Sensing Letters · October 2017

DOI: 10.1109/LGRS.2017.2755061

CITATIONS
74

READS
526

6 authors, including:

Haoyang Yu
Dalian Maritime University
50 PUBLICATIONS **671** CITATIONS

SEE PROFILE

Lianru Gao
CAS
252 PUBLICATIONS **8,481** CITATIONS

SEE PROFILE

Wenzhi Liao
Ghent University
118 PUBLICATIONS **4,956** CITATIONS

SEE PROFILE

Multiscale Superpixel-Level Subspace-Based Support Vector Machines for Hyperspectral Image Classification

Haoyang Yu, *Student Member, IEEE*, Lianru Gao, *Member, IEEE*, Wenzhi Liao, *Senior Member, IEEE*, Bing Zhang, *Senior Member, IEEE*, Aleksandra Pižurica, *Senior Member, IEEE*, and Wilfried Philips, *Senior Member, IEEE*

***Abstract*— This letter introduces a new spectral–spatial classification method for hyperspectral images. A multiscale superpixel segmentation is first used to model the distribution of classes based on spatial information. In this context, the original hyperspectral image is integrated with segmentation maps via a feature fusion process in different scales such that the pixel-level data can be represented by multiscale superpixel-level (MSP) data sets. Then, a subspace-based support vector machine (SVMsub) is adopted to obtain the classification maps with multiscale inputs. Finally, the classification result is achieved via a decision fusion process. The resulting method, called MSP-SVMsub, makes use of the spatial and spectral coherences, and contributes to better feature characterization. Experimental results based on two real hyperspectral data sets indicate that the MSP-SVMsub exhibits good performance compared with other related methods.**

***Index Terms*— Hyperspectral image classification, multiscale superpixel segmentation, subspace projection, support vector machines (SVM).**

I. Introduction

RECENT advances in hyperspectral imaging sensors allow us to acquire hyperspectral data with increasing spectral resolution, benefiting the precision land-use and land-cover mapping. In order to better characterize the image for classification, it is reasonable to integrate different types of features in spectral and spatial domains. Object-based image classification (OBIC) is one of the well-established frameworks including spatial information for classification [1]. It performs classification after segmentation, and each segment is regarded as a homogeneous unit in the classification process. Segmentation techniques divide an image into several nonoverlapping homogeneous regions based on different spectral characteristics. Segmentation methods have shown effective results for hyperspectral images including watershed segmentation, thresholding, and partitional clustering [2], [3]. Actually, it has been proved that each segment can also be regarded as a superpixel, which is part of an object [4]. Oversegmentation is often adopted to obtain the superpixel to represent the local information and exploit the spatial correlation [5]. Gao *et al.* [6] propose a discriminative classifier based on the decision forest using the features at both pixel and superpixel levels, which perform better segmentation in some cases. Jia *et al.* [7] integrate the pixelwise sparse representation classification with superpixel-level segmentation, which brings considerable improvement to the original counterparts. However, most of these OBIC-based methods typically perform on a single fixed scale, which causes the result to suffer from finding an optimal scale. The actual situation is that the optimal scale for image segmentation generally differs for different classes in a remote sensing scene [8]. It is not appropriate to select a single random or fixed segmentation scale for all the classes. Therefore, it is desirable to establish a multiscale OBIC framework for the comprehensive utilization of image information.

Hyperspectral images are characterized by their high spectral resolution, but it also has been demonstrated that the original spectral features contain high redundancy and correlation between the adjacent bands [9]. The imbalance between the high dimensionality of features and limited training sample size has been the main constraint of hyperspectral image classification, i.e., Hughes phenomenon. In this context, subspace projection has shown to be a powerful technique for feature exploitation and dimensionality reduction [10]. The fundamental idea of such a method is to project the original pixel vector to a lower dimensional subspace, which is spanned by a set of basis vectors. It is useful for reducing the dimensionality without loss of information, and also suitable for the partition of classes that are spectrally similar by spectral mixing or other reasons [11]. Recently, several subspace-based methods have been proposed for hyperspectral image classification [12]. Li *et al.* [13] integrate subspace-based multinomial logistic regression with MRF, which performs

Manuscript received September 1, 2017; accepted September 12, 2017. This work was supported by the National Natural Science Foundation of China under Grant 41722108, Grant 41325004, and Grant 91638201. *(Corresponding author: Lianru Gao.)*

H. Yu and B. Zhang are with the Key Laboratory of Digital Earth Science, Institute of Remote Sensing and Digital Earth, Chinese Academy of Sciences, Beijing 100094, China, and also with the College of Resources and Environment, University of Chinese Academy of Sciences, Beijing 100049, China (e-mail: yuhy@radi.ac.cn; zb@radi.ac.cn).

L. Gao is with the Key Laboratory of Digital Earth Science, Institute of Remote Sensing and Digital Earth, Chinese Academy of Sciences, Beijing 100094, China (e-mail: gaolr@radi.ac.cn).

W. Liao, A. Pižurica, and W. Philips are with the Department of Telecommunications and Information Processing, IMEC-TELIN-Ghent University, 9000 Ghent, Belgium (e-mail: wliao@telin.ugent.be; aleksandra.pizurica@telin.ugent.be; wilfried.philips@telin.ugent.be).

Color versions of one or more of the figures in this letter are available online at http://ieeexplore.ieee.org.

Digital Object Identifier 10.1109/LGRS.2017.2755061

better characterization of information and segmentation of image. Gao *et al.* [14] combine the subspace projection and support vector machines (SVMs) to bring more reliable and robust classification performances with a relatively low computational cost.

Inspired by the previous approaches, this letter presents a multiscale superpixel-level subspace-based SVM (MSP-SVMsub) for hyperspectral image classification. The proposed method, MSP-SVMsub, is implemented into three steps. First, the simple linear iterative clustering (SLIC) method is used to obtain the superpixel to segment the original hyperspectral image into different scales [15]. By applying a feature fusion process, the original spectral features can be integrated with the multiscale spatial features such that the pixel-level data is represented by MSP data sets. Then, SVMsub is adopted to obtain the classification maps by using fusion features from different scales as the inputs. The final classification result is achieved by decision fusion of the resulting maps obtained by multiscale classifiers.

The main contribution of the proposed approach is the integration of multiscale superpixel segmentation with SVMsub, which solves the problem of classic OBIC-based methods suffering from finding the optimal segmentation scale and the Hughes phenomenon in hyperspectral image classification.

II. Proposed Classification Framework

Given a hyperspectral image denoted as $\mathbf{X} \equiv \{\mathbf{x}_1, \mathbf{x}_2, \ldots, \mathbf{x}_n\}$ with n pixels, where $\mathbf{x}_i = \{x_{i,b} | i = 1, \ldots, n, b = 1, \ldots, B\}$ represents the value of pixel i in spectral band b, and B is the number of spectral bands. The corresponding labels can be denoted as $\mathbf{y} \equiv \{y_1, y_2, \ldots, y_n\}$, where $\mathbf{y}_i \in \{-1, 1\}$. For a label set $C \equiv \{1, \ldots, K\}$, where K is the total class number, if pixel i belongs to class c, we say $y_i^{(c)} = 1$; otherwise, $y_i^{(w)} = -1$ for $w \in \{C | w \neq c\}$.

A. Superpixel Segmentation

OBIC performs classification on object (grouped by several pixels) instead of per-pixel. By this way, OBIC can better exploit the spatial information of the image, as well as reduce the computational costs and for the post land-use/land-cover or change detection mapping project. Superpixel segmentation (SLIC) is one of the most widely used methods to segment an image into objects, due to its low computational complexity by applying the k-means method locally [15]. The algorithm starts with selecting T cluster centers in the original scene, and an iterative clustering process is performed until the change of the cluster center tends to be stable. Unlike the k-means, of which the distance is defined from each cluster center to every pixel in the image, SLIC only computes distances within a size of $2S \times 2S$ region around the superpixel center, where $S = \sqrt{n/T}$. Specifically, the distance is defined as follows:

$$D = D_{\text{spectral}} + \frac{m}{h} D_{\text{spatial}} \tag{1}$$

where m is the geometric parameter and h is the scale parameter, which controls the number and size of the superpixel. D_{spectral} is the spectral measure term to control the homogeneity within a superpixel and D_{spatial} is the spatial measure term to ensure the regularity and compactness. The spectral and spatial distances between pixel i and j are defined as follows:

$$D_{\text{spectral}} = \sqrt{\sum_{b=1}^{B} (x_{i,b} - x_{j,b})^2} \tag{2}$$

$$D_{\text{spatial}} = \sqrt{(p_i - p_j)^2 + (q_i - q_j)^2} \tag{3}$$

where (p_i, q_i) represent the location of pixel i in the superpixel. Since the original SLIC is mainly performed for color images in the CIELAB color space, the input need to be represented as $\mathbf{x}_i = (l_i, a_i, b_i)$. Therefore, it is suggested that preprocessing like principle component analysis (PCA) can be adopted to obtain the first three components such that the original hyperspectral data can be processed by SLIC [5], [8].

B. Subspace-Based SVM

The hyperspectral data can be considered to live on a lower dimensional class-dependent subspace under the linear mixture model assumption [12]. Therefore, for any pixel i, one has

$$\mathbf{x}_i = \sum_{c=1}^{k} \mathbf{U}^{(c)} \mathbf{z}_i^{(c)} + \mathbf{n}_i \tag{4}$$

where $\mathbf{U}^{(c)} = \{\mathbf{u}_1^{(c)}, \ldots, \mathbf{u}_{r^{(c)}}^{(c)}\} \in \mathbf{R}^{B \times r^{(c)}}$ is a set of orthonormal basis vectors for the subspace, $\mathbf{z}_i^{(c)}$ represents the corresponding coordinates of $\mathbf{x}_i$, and $\mathbf{n}_i$ is the noise. Considering $G = \{G^{(1)}, \ldots, G^{(k)}\}$ to be the set of labeled training data of each class, where $G^{(c)} = \{\mathbf{x}_1^{(c)}, \ldots, \mathbf{x}_{l^{(c)}}^{(c)}\}$ denotes the set of samples with label c and size $l^{(c)}$, the matrix $\mathbf{R}^{(c)} = G^{(c)} G^{(c)T}$ can be transformed into $\mathbf{R}^{(c)} = \mathbf{E}^{(c)} \mathbf{\Lambda}^{(c)} \mathbf{E}^{(c)T}$, where $\mathbf{E}^{(c)} = \{\mathbf{e}_1^{(c)}, \ldots, \mathbf{e}_B^{(c)}\}$ is the eigenvector and $\mathbf{\Lambda} = \text{diag}(\lambda_1^{(c)}, \ldots, \lambda_B^{(c)})$ contains the eigenvalues of $\mathbf{R}^{(c)}$ with decreasing magnitudes. Following [12], $r^{(c)}$ is defined to retain 99% of the original spectral information, i.e., $r^{(c)} = \min\{r^{(c)} | \sum_{i=1}^{r^{(c)}} \lambda_i^{(c)} \geq \sum_{i=1}^{B} \lambda_i^{(c)} \times 99\%\}$, such that $\mathbf{U}^{(c)} = \{\mathbf{e}_1^{(c)}, \ldots, \mathbf{e}_{r^{(c)}}^{(c)}\}$ can be adopted as the basis of the subspace. In this way, $\mathbf{x}_i$ can be projected to this class-dependent subspace, and the transformed pixel can be defined by a nonlinear function as

$$\phi(\mathbf{x}_i) = [\|\mathbf{x}_i\|^2, \|\mathbf{x}_i \mathbf{U}^1\|^2, \ldots, \|\mathbf{x}_i \mathbf{U}^K\|^2]^T. \tag{5}$$

Here, we need to note that subspace projection is not a PCA method. It is a nonlinear projection technique, which relies on the basic assumption that samples can approximately lie in a lower dimensional subspace. Unlike the result of PCA, which is sorted according to the amount of information, the criterion of subspace projection is the distance from the class subspace spanned by a set of basic vectors from the training set.

On the other hand, the selection of the particular classifier is crucial for the performance of classification, especially due to the problem of a small training sample size in hyperspectral images. Among the various classifiers in the spectral domain, SVM is a widely used supervised statistical learning framework. The main principle of SVM is to find the optimal

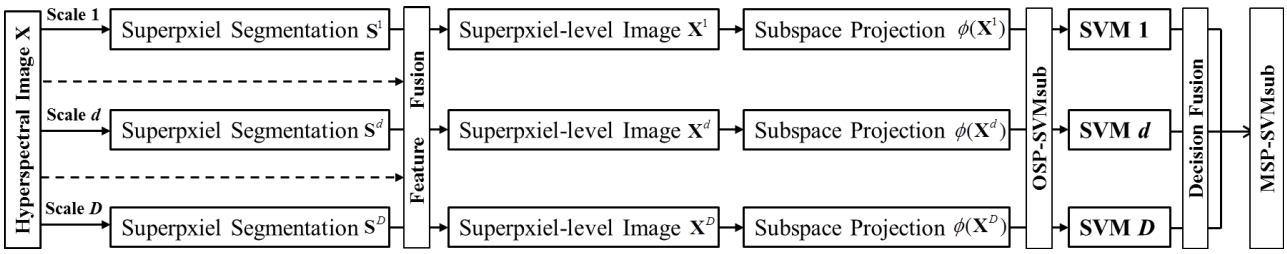

Fig. 1. Framework for MSP-SVMsub.

hyperplane, which separates samples belonging to different classes, such that the distance between the hyperplane and the closest training sample to it is maximized [10]. The decision rule of the classical linear SVM classifier for pixel i can be expressed as

$$y_i = \operatorname{sgn}\left(\sum_{j=1}^{l_n} y_j \alpha_j \left(\mathbf{x}_j^T \mathbf{x}_i\right) + \beta\right) \tag{6}$$

where l_n is the size of labeled samples. In practice, linear separability is usually hard to satisfy, since the basic linear decision boundaries are often insufficient to model the data. Therefore, a kernel method has been introduced to cope with the nonseparable scenarios by mapping the data via a nonlinear transformation to another feature space.

In this context, it is feasible to integrate the subspace projection with the SVM classifier. Based on the aforementioned techniques, the SVMsub can be expressed with the transformed data $\phi\ (\mathbf{X}) \equiv \{\phi\ (\mathbf{x}_1), \ldots, \phi\ (\mathbf{x}_n)\}$ as follows:

$$y_i = \operatorname{sgn}\left(\sum_{j=1}^{l_n} y_j \alpha_j (\phi(\mathbf{x}_j)^T \phi(\mathbf{x}_i)) + \beta\right). \tag{7}$$

C. Multiscale Superpixel-Level SVMsub

As illustrated in Fig. 1, spatial features are explored by multiscale superpixel segmentation, whereas spectral features are utilized by subspace projection. Specifically, let $\mathbf{S}^d$ be the superpixel segmentation map at scale $d \in (1, \ldots, D)$, and the mean vector $\mathbf{m}_l^d$ of the corresponding region in $\mathbf{X}$ to the lth superpixel in $\mathbf{S}^d$ can be calculated to replace all the spectral feature of pixels in this region. Therefore, the pixel-level data $\mathbf{X}$ can be transformed into the superpixel-level data $\mathbf{X}^d$, and then $\mathbf{X}^d$ is adopted as the new input to the SVMsub implementation. The above process can also be called one-scale superpixel-level SVMsub (OSP-SVMsub).

After performing OSP-SVMsub at each scale, a decision fusion process of majority voting is adopted to obtain the final classification map of MSP-SVMsub, where the class of each pixel is determined by the maximum number of labels in the corresponding location of each scale. The pseudocode for the MSP-SVMsub is provided in Algorithm 1.

Algorithm 1 MSP-SVMsub

Input: Available training data $\mathbf{X} = \{\mathbf{x}_i\}_{i=1}^n$ and a testing sample set with class labels represented by $\mathbf{y}$.

Step 1: Obtain the multi-scale superpixel segmentation maps $\mathbf{S}^D = \{\mathbf{S}^d\}_{d=1}^D$ of $\mathbf{X}$ according to Equation (1) $\sim$ (3).

Step 2: Obtain $\mathbf{X}^D = \{\mathbf{X}^d\}_{d=1}^D$ via the fusion of $\mathbf{S}^D$ and $\mathbf{X}$ according to OSC.

Step 3: Obtain the transformed $\phi\ (\mathbf{X}^D) = \{\phi\ (\mathbf{X}^d)\}_{d=1}^D$ according to Equation (4) $\sim$ (5).

Step 4: Compute the class label $\mathbf{y}^D = \{\mathbf{y}^d\}_{d=1}^D$ with $\phi\ (\mathbf{X}^D)$ according to Equation (7)

Step 5: Determine the final class label.

$$class(\mathbf{y}) = \arg \underset{d=1,\ldots D}{\operatorname{mod}} class(\mathbf{y}^d)$$

Output: The class labels $\mathbf{y}$.

III. Experimental Results

In this section, the proposed MSP-SVMsub is evaluated with two real hyperspectral data sets. The first one is collected by the Airborne Visible/Infrared Imaging Spectrometer (AVIRIS) over the Indian Pines region in June 1992. The scene contains 145×145 pixels, with 220 spectral bands in the spectral range from 0.4 to 2.5 μm and a nominal spectral resolution of 10 nm. The ground reference contains 16 mutually exclusive classes, with a total of 10 366 labeled samples. The other one is collected by the Reflective Optics System Imaging Spectrometer (ROSIS) over the University of Pavia, Italy, in 2001. The scene contains 610×340 pixels, with 103 spectral bands in the spectral range from 0.43 to 0.86 μm, after removing 12 bands of noise and water absorption. The ground reference contains a total of 3921 training samples and 42 776 test samples belonging to nine classes. As for parameter tuning, considering the principle of decision fusion and the issue of undersegmentation, the segmentation is generally selected at seven scales $D = \{n/s, s = 5, 10, 15, 25, 50, 75, 100\}$ for two data sets, where n denotes the total number of pixels. For comparative purpose, several related well-established spectral and spectral–spatial methods are considered in this letter, such as SVM, SVMsub, SVM-MRF, and SVMsub-MRF [11], [14]. In addition, we develop the OSP-SVM, OSP-SVMsub, and MSP-SVM as comparisons to evaluate the proposed MSP-SVMsub. The parameters of different methods have been carefully optimized by means of fivefold cross-validation according to the procedure described in the literature. Each value of overall accuracy (OA) and κ statistic is provided after 20 Monte Carlo runs with respect to the same number of randomly selected labeled samples per class.

For the AVIRIS Indian Pines hyperspectral scene, we evaluate the proposed MSP-SVMsub with different training size (from 10 to 50 samples per class). As reported in Table I,

Fig. 2. Classification maps of different tested methods for the AVIRIS Indian Pines scene (30 samples per class).

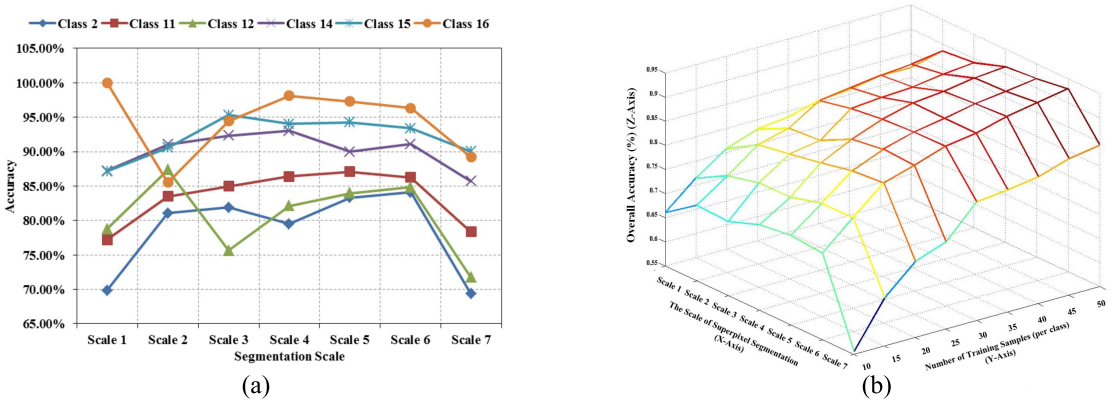

(a) (b)

Fig. 3. Sensitivity analysis of the scale of superpixel segmentation of OSP-SVMsub for the AVIRIS Indian Pines scene. (a) Segmentation scale versus individual class (30 samples per class). (b) Segmentation scale versus training size.

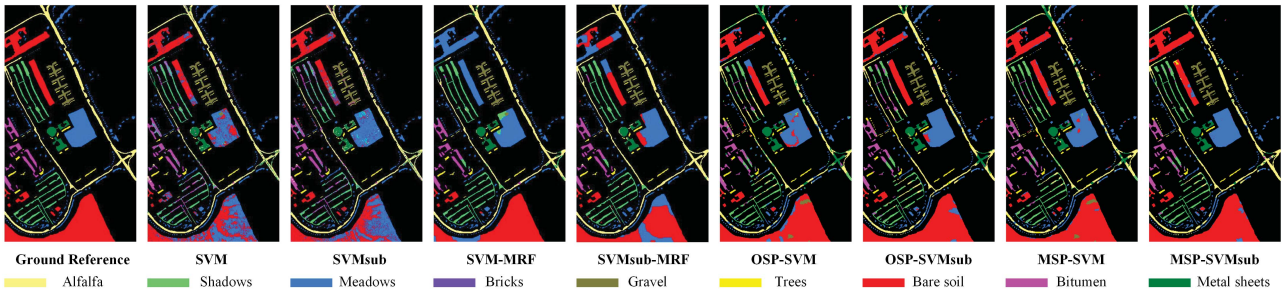

Fig. 4. Classification maps of different tested methods for the ROSIS University of Pavia scene (20 samples per class).

several conclusions can be summarized as follows.

1) Classification accuracy is generally positively correlated with the number of training samples.
2) Subspace projection technique contributes to better exploit the feature for classification, especially for the situation of limited training samples, which can be proved by the OA and its variation trend between subspace-based methods and their original counterparts.
3) The integration with contextual information helps to better characterize the image in the spectral–spatial domain based on the result of the MRF-based methods and the superpixel-level methods versus their original counterparts.
4) Object-based methods make more comprehensive consideration of spatial and spectral coherences compared with the pixel-based classification results.

For illustrative purpose, Fig. 2 shows the corresponding classification maps of 30 training samples per class. It is clear that spectral–spatial methods, especially MSP-SVMsub, provide better performances than does the spectral ones with respect to the influence of noise and mixed pixels.

Fig. 3(a) shows the individual class accuracy obtained by six representative classes, as a function of the segmentation scale (using 30 training samples per class). As illustrated, for different classes, the optimal segmentation scale is different. Especially for some large and widely distributed classes like class 2 and 11, their optimal scales appear to be very different from those smaller classes like class 16. On the other hand, Fig. 3(b) shows the relationship between OA, segmentation scale, and the number of training samples. As illustrated, the OAs of OSP-SVMsub at different scales generally increase with the training size, which can be seen from the *YZ* plane. Most importantly, for a certain number of training samples, the optimal scale of superpixel segmentation is also different, which can be seen from the *XZ* plane. Therefore, it may be not appropriate to select a random or fixed segmentation scale for OBIC. By taking into account different scales of various objects, the proposed MSP-SVMsub achieves better performances than does the other methods, which proves the usefulness of our approach.

In the experiment with the ROSIS University of Pavia scene, we also evaluate the proposed method with different training sizes (from 10 to 100 samples per class). As reported in Table II, similar conclusions can be obtained with the Indian Pines's experiment. The difference is that the integration with spatial information contributes more than that with subspace

TABLE I

OA AND κ STATISTIC (IN PARENTHESES) WITH DIFFERENT NUMBERS OF TRAINING SAMPLES FOR THE AVIRIS INDIAN PINES SCENE

Sample (per class)	SVM	SVMsub	SVM-MRF	SVMsub-MRF	OSP-SVM	OSP-SVMsub	MSP-SVM	MSP-SVMsub
160 (10)	38.98% (0.33)	53.75% (0.48)	50.59% (0.46)	67.49% (0.63)	67.77% (0.64)	72.91% (0.69)	76.31% (0.73)	80.48% (0.78)
240 (15)	44.56% (0.39)	58.23% (0.53)	58.03% (0.54)	74.86% (0.72)	73.87% (0.70)	78.49% (0.76)	83.44% (0.81)	84.01% (0.82)
320 (20)	51.83% (0.46)	61.87% (0.57)	72.58% (0.69)	79.82% (0.77)	78.47% (0.76)	83.99% (0.82)	87.95% (0.86)	90.74% (0.89)
400 (25)	55.30% (0.50)	65.27% (0.61)	77.64% (0.75)	82.09% (0.80)	81.88% (0.79)	85.87% (0.84)	89.73% (0.88)	91.47% (0.90)
480 (30)	57.81% (0.53)	68.63% (0.64)	80.50% (0.78)	84.69% (0.83)	83.99% (0.82)	88.03% (0.86)	90.36% (0.89)	92.41% (0.91)
560 (35)	60.33% (0.55)	69.79% (0.66)	82.50% (0.80)	86.39% (0.84)	85.71% (0.84)	88.98% (0.87)	91.31% (0.90)	93.68% (0.93)
640 (40)	61.45% (0.57)	71.34% (0.67)	83.43% (0.81)	87.98% (0.86)	88.12% (0.86)	90.65% (0.89)	92.11% (0.91)	94.43% (0.94)
720 (45)	62.48% (0.58)	72.56% (0.69)	84.92% (0.83)	88.08% (0.86)	88.47% (0.87)	91.84% (0.91)	92.69% (0.92)	95.13% (0.94)
800 (50)	64.19% (0.59)	74.11% (0.70)	86.36% (0.84)	90.07% (0.89)	90.08% (0.89)	92.91% (0.92)	93.58% (0.93)	95.28% (0.95)

TABLE II

OA AND κ STATISTIC (IN PARENTHESES) WITH DIFFERENT NUMBERS OF TRAINING SAMPLES FOR THE ROSIS UNIVERSITY OF PAVIA

Sample (per class)	SVM	SVMsub	SVM-MRF	SVMsub-MRF	OSP-SVM	OSP-SVMsub	MSP-SVM	MSP-SVMsub
180 (20)	70.82% (0.64)	71.99% (0.65)	78.03% (0.73)	81.36% (0.77)	79.66% (0.74)	85.32% (0.81)	87.98% (0.84)	91.90% (0.89)
270 (30)	73.87% (0.67)	74.27% (0.68)	84.34% (0.81)	85.14% (0.82)	83.60% (0.79)	88.29% (0.85)	90.34% (0.87)	93.83% (0.92)
360 (40)	77.26% (0.71)	77.30% (0.71)	87.01% (0.84)	87.31% (0.84)	88.30% (0.85)	90.92% (0.88)	92.81% (0.90)	94.94% (0.93)
450 (50)	78.28% (0.72)	78.74% (0.73)	88.62% (0.86)	88.64% (0.86)	88.25% (0.85)	91.82% (0.89)	94.28% (0.92)	96.13% (0.95)
540 (60)	79.85% (0.74)	81.33% (0.76)	89.53% (0.87)	90.33% (0.88)	90.63% (0.88)	93.31% (0.91)	93.87% (0.92)	96.78% (0.96)
630 (70)	80.70% (0.75)	81.59% (0.76)	90.04% (0.88)	90.76% (0.89)	90.83% (0.88)	93.13% (0.91)	95.32% (0.94)	97.03% (0.96)
720 (80)	81.29% (0.76)	81.68% (0.77)	91.34% (0.89)	92.11% (0.90)	92.25% (0.90)	94.57% (0.93)	95.60% (0.94)	97.53% (0.97)
810 (90)	82.24% (0.77)	82.45% (0.77)	92.16% (0.90)	92.36% (0.91)	92.91% (0.91)	95.05% (0.93)	95.71% (0.94)	97.33% (0.96)
900 (100)	83.21% (0.78)	83.23% (0.78)	92.19% (0.90)	92.74% (0.91)	93.00% (0.91)	95.21% (0.94)	96.07% (0.95)	97.57% (0.97)

projection for the University of Pavia, which is mainly due to the fact that the Hughes phenomenon here is not as obvious as in the case of Indian Pines. In general, MSP-SVMsub still obtains better results in terms of both the OA and κ statistic than other related methods in all cases. For instance, as illustrated in Fig. 4, when a total of 180 training samples are used (approximately 0.4% of the labeled samples), MSP-SVMsub obtains the best result with an OA of 91.90%, which is 19.91% and 6.58% higher than those for SVMsub and OSP-SVMsub, respectively. The above results and analysis show convincingly the effectiveness and reliability of the proposed MSP-SVMsub method.

IV. CONCLUSION

In this letter, an MSP-SVMsub classifier was proposed for hyperspectral image classification. The main contributions include fusing multiscale superpixel segmentation with SVMsub in spectral–spatial domain, solving the problem of classic OBIC-based methods suffering from finding the optimal segmentation scale and the Hughes phenomenon in hyperspectral image classification. The proposed method has been compared with the classical SVM, SVMsub, and their integration with other spatial frameworks using two real hyperspectral data sets. The experimental results demonstrated that an MSP-SVMsub outperformed the original counterparts and their variants, and yielded better classification performances.

REFERENCES

[1] H. Sridharan and F. Qiu, "Developing an object-based hyperspatial image classifier with a case study using WorldView-2 data," *Photogramm. Eng. Remote Sens.*, vol. 79, no. 11, pp. 1027–1036, Nov. 2013.

[2] M. Fauvel, Y. Tarabalka, J. A. Benediktsson, J. Chanussot, and J. C. Tilton, "Advances in spectral-spatial classification of hyperspectral images," *Proc. IEEE*, vol. 101, no. 3, pp. 652–675, Mar. 2013.

[3] X. Zhang, C. Xu, M. Li, and X. Sun, "Sparse and low-rank coupling image segmentation model via nonconvex regularization," *Int. J. Pattern Recognit. Artif. Intell.*, vol. 29, no. 2, p. 1555004, Jan. 2015.

[4] S. Li, X. Jia, and B. Zhang, "Superpixel-based Markov random field for classification of hyperspectral images," in *Proc. IEEE Int. Geosci. Remote Sens. Symp. (IGARSS)*, Jul. 2013, pp. 3491–3494.

[5] S. Jia, B. Deng, J. Zhu, X. Jia, and Q. Li, "Superpixel-based multitask learning framework for hyperspectral image classification," *IEEE Trans. Geosci. Remote Sens.*, vol. 55, no. 5, pp. 2575–2588, May 2017.

[6] Q. Gao, A. Asthana, T. Tong, D. Rueckert, and P. E. Edwards, "Multi-scale feature learning on pixels and super-pixels for seminal vesicles MRI segmentation," *Proc. SPIE*, vol. 9034, p. 903407, Mar. 2014.

[7] S. Jia, B. Deng, and X. Jia, "Superpixel-level sparse representation-based classification for hyperspectral imagery," in *Proc. IEEE Int. Geosci. Remote Sens. Symp. (IGARSS)*, Jul. 2016, pp. 3302–3305.

[8] S. Li, L. Ni, X. Jia, L. Gao, B. Zhang, and M. Peng, "Multi-scale superpixel spectral–spatial classification of hyperspectral images," *Int. J. Remote Sens.*, vol. 37, no. 20, pp. 4905–4922, Sep. 2016.

[9] Y. Qian, F. Yao, and S. Jia, "Band selection for hyperspectral imagery using affinity propagation," *IET Comput. Vis.*, vol. 3, no. 4, pp. 213–222, Dec. 2009.

[10] W.-S. Chen, J. Huang, J. Zou, and B. Fang, "Wavelet-face based subspace LDA method to solve small sample size problem in face recognition," *Int. J. Wavelets, Multiresolution Inf. Process.*, vol. 7, no. 2, pp. 199–214, Mar. 2009.

[11] H. Yu, L. Gao, J. Li, S. S. Li, B. Zhang, and J. A. Benediktsson, "Spectral-spatial hyperspectral image classification using subspace-based support vector machines and adaptive Markov random fields," *Remote Sens.*, vol. 8, no. 4, p. 355, Apr. 2016.

[12] Z. Zhu, S. Jia, S. He, Y. Sun, Z. Ji, and L. Shen, "Three-dimensional Gabor feature extraction for hyperspectral imagery classification using a memetic framework," *Inf. Sci.*, vol. 298, pp. 274–287, Mar. 2015.

[13] J. Li, J. M. Bioucas-Dias, and A. Plaza, "Spectral–spatial hyperspectral image segmentation using subspace multinomial logistic regression and Markov random fields," *IEEE Trans. Geosci. Remote Sens.*, vol. 50, no. 3, pp. 809–823, Mar. 2012.

[14] L. Gao *et al.*, "Subspace-based support vector machines for hyperspectral image classification," *IEEE Geosci. Remote Sens. Lett.*, vol. 12, no. 2, pp. 349–353, Feb. 2015.

[15] R. Achanta, A. Shaji, K. Smith, A. Lucchi, P. Fua, and S. Süsstrunk, "SLIC superpixels compared to state-of-the-art superpixel methods," *IEEE Trans. Pattern Anal. Mach. Intell.*, vol. 34, no. 11, pp. 2274–2282, Nov. 2012.